

Signatures of oxygen on Cu₃Au(100): From isolated impurity to oxide regimes

Alexandre A. Leitão,^{1,2,*} L. G. Dias,³ M. Dionízio Moreira,² F. Stavale,^{2,4} H. Niehus,^{2,5} C. A. Achete,^{2,4} and Rodrigo B. Capaz^{2,6}

¹Departamento de Química, Universidade Federal de Juiz de Fora, Juiz de Fora 36036-330, MG, Brazil

²Divisão de Metrologia de Materiais (DIMAT), Instituto Nacional de Metrologia, Normalização e Qualidade Industrial, Av. N. Sra. das Graças 50, Xerém, Duque de Caxias CEP 25250-020, RJ, Brazil

³Departamento de Química, FFCLRP, Universidade de São Paulo, Ribeirão Preto 14040-901, SP, Brazil

⁴Engenharia Metalúrgica e de Materiais, Universidade Federal do Rio de Janeiro, Caixa Postal 68505, Rio de Janeiro CEP 21945-970, RJ, Brazil

⁵Institut für Physik, Oberflächenphysik und Atomstoßprozesse, Humboldt-Universität zu Berlin, Newtonstr. 15, D-12489 Berlin, Germany

⁶Instituto de Física, Universidade Federal do Rio de Janeiro, Caixa Postal 68528, Rio de Janeiro 21941-972, RJ, Brazil

(Received 19 March 2010; revised manuscript received 15 June 2010; published 9 July 2010)

We analyze the scanning tunneling microscopy (STM) signatures for the O/Cu₃Au(100) surface from the low-coverage (isolated impurity) to high-coverage (oxide) regimes. First-principles calculations show that oxygen signatures switch from dark to bright spots as the oxygen coverage increases. This behavior is nicely traced back to a change in the oxygen orbital character of the Fermi-level electronic states. Our results allow for the chemical identification by STM of oxygen and copper atoms in the fully ordered O/Cu₃Au(100)- $c(2 \times 2)$ surface.

DOI: [10.1103/PhysRevB.82.045408](https://doi.org/10.1103/PhysRevB.82.045408)

PACS number(s): 68.37.Ef, 73.20.At

I. INTRODUCTION

The study of oxygen on metallic surfaces is important from both fundamental and technological points of view. Oxygen atoms can be present in different concentrations on the surface, ranging from very small amounts (isolated-impurity limit) to a full coverage of chemisorbed oxygen in the monolayer regime and then finally to three-dimensional oxide growth. In the high-coverage limit, the surface can be rather viewed as a metal oxide, and the chemical identification of the oxygen atoms using tools such as scanning tunneling microscopy (STM) may not be a trivial task.

Copper and its alloys have wide industrial applications and there is the interest for studies of oxidation mechanisms, especially pertinent in Cu₂O formation.^{1,2} In particular, Cu₃Au as an ordered alloy has a cubic L₁₂ structure and low-energy electron diffraction (LEED), ion-scattering spectroscopy, and STM data for the (100) surface suggest that it has Au-rich terminations, with Au 50% and Cu 50%, and Cu-rich second layer, with 100% Cu.³ Recent *ab initio* calculations based on density-functional theory (DFT) of the surface energy as a function of the Cu chemical potential have confirmed these results⁴ and have provided chemical identification of Au and Cu atoms at the surface.

Recently, we have reported that well-ordered transition-metal oxide films on a metallic substrate can be prepared by using a Cu₃Au(100) substrate with implanted oxygen (CAOS, Cu₃Au-oxygen substrate).⁵ Because the Cu₃Au(100) surface appears virtually inert against molecular oxygen adsorption, the initial procedure in this technique is the implantation of O atoms by sputtering using 200 eV O⁺. After healing out the sputter defects and by that restructuring the surface area by subsequent annealing, a flat and a well-ordered O/Cu₃Au(100)- $c(2 \times 2)$ surface is formed. This oxygen-rich Cu₃Au surface [oxygen atom coverage of 1/2 monolayer (ML)] was first studied by Niehus and Achete³

using ion scattering, LEED, STM, and direct recoil spectroscopy. They found that, after saturation with oxygen, the surface is no longer terminated by the CuAu plane but instead by the Cu plane with oxygen adsorbed in the fourfold hollow sites above subsurface Cu atoms and by that also maintaining the $c(2 \times 2)$ symmetry [see Fig. 1(a)]. This result is consistent with the idea that Cu forms a stable Cu₂O oxide while Au does not. Similarly, Okada *et al.*^{1,2} obtained the same oxygen coverage on Cu₃Au(100) using a hyperthermal O₂ molecular beam. After such a treatment, an oxygen-induced Cu segregation has been reported.

The STM images of the O/Cu₃Au(100)- $c(2 \times 2)$ surface reveal the surface periodicity by a network of bright protrusions.³ However, chemical identification of oxygen or copper sites has not been achieved so far. For other metals or metal alloys, in the single-impurity or low-concentration limit, atomic oxygen usually produces dark spots in the scanning tunneling microscopy images.⁶ For instance, in the work of Wiame *et al.*,⁷ for the initial stages of oxygen adsorption on Cu(111), the appearance of dark spots (depres-

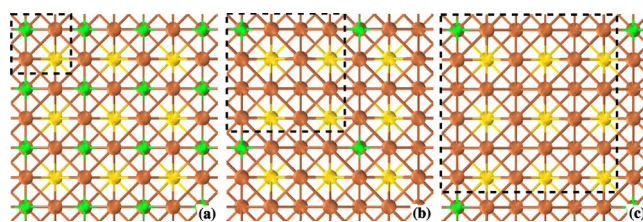


FIG. 1. (Color online) Top view for (a) 1/2 ML, (b) 1/8 ML, and (c) 1/18 ML oxygen atom coverage on Cu₃Au(100). Green, yellow, and bronze balls represent oxygen, gold, and copper, respectively. Both first-layer and second-layer atoms can be seen. All gold atoms belong to the second atomic layer and oxygen sits in hollow sites of the first layer, on top of second-layer copper atoms. The areas marked with dashed lines represent the surface unit cell in each case.

sions) with C_3 local symmetry was reported, which were attributed to oxygen atoms occupying threefold hollow sites at the surface. Similarly, STM experiments for low oxygen-atom coverage on Cu(100) also show isolated dark spots.⁸ Therefore, one could be tempted to assign the bright spots of the O/Cu₃Au(100)- $c(2 \times 2)$ surface to the Cu atoms and the dark spots to O atoms. Indeed, for the related O/Cu(100)- $c(2 \times 2)$ surface, previous STM studies have tentatively assigned the dark spots in the images to oxygen atoms.⁹

In this work, we show that bright spots in the STM images of the O/Cu₃Au(100)- $c(2 \times 2)$ actually correspond to oxygen atoms. In particular, they are assigned to electronic states near the Fermi level with a large component of oxygen p_z orbitals sticking out of the surface. As the oxygen concentration gradually decreases, the oxygen orbital character of the Fermi-level states changes from p_z to (p_x , p_y), and then the oxygen atoms appear as dark spots in the isolated-impurity limit.

II. EXPERIMENTAL SETUP

All experiments were carried out in ultrahigh vacuum (base pressure 5×10^{-11} mbar), following the CAOS method⁵ to create a flat Cu₃Au(100)-oxygen surface³ by oxygen implantation and subsequent annealing. The ultrahigh-vacuum system is equipped with variable-temperature STM (OMICRON), LEED, and Auger-electron spectroscopy (AES) facilities. The Cu₃Au(100) was initially treated by several cycles of 1 keV Ar⁺ sputtering at room temperature and subsequent annealing at 800 K, until no detectable impurities were found with AES. Thereafter, the sample was held overnight at about 650 K followed by slow cool down to room temperature in order to allow bulk and surface ordering getting complete. The resulting LEED pattern then showed a $c(2 \times 2)$ superstructure with sharp LEED spots, typical of the clean Cu₃Au(100) surface. Then the crystal was sputtered by oxygen at room temperature ($E=500$ eV, $P_{O_2} < 2 \times 10^{-5}$ mbar, 30 min). Subsequent annealing at $T > 650$ K (5 min) drives oxygen out of the bulk toward the surface, healing out all sputtering defects and forming the ordered O/Cu₃Au(100)- $c(2 \times 2)$ structure. All STM images were acquired at room temperature by the use of etched tungsten tips in the constant current mode.

III. THEORETICAL METHODOLOGY

Our *ab initio* DFT (Refs. 10 and 11) calculations are based on the local-density approximation using periodic boundary conditions. We adopt the exchange-correlation functional parametrized by Perdew and Zunger.¹² We use ultrasoft pseudopotentials¹³ and a plane-wave basis with maximum kinetic energy of 40 Ry, as implemented by the PWSCF code.¹⁴ Valence shells with 11, 11, and 6 electrons were considered for Cu, Au, and O, respectively.

The clean Cu₃Au(100) surface is modeled by a symmetric slab geometry with five layers. The slabs consist of two layers with Cu:Au 1:1 and three Cu planes (one at the slab center and two at the surfaces). The lateral lattice parameter

of the supercell was kept fixed at the theoretical bulk value (7.08 bohrs). Along the axis perpendicular to the surface, a large (56 bohrs) lattice constant was used as to provide a substantial vacuum region. Three models were prepared to investigate 1/2, 1/8, and 1/18 ML of oxygen atoms on Cu₃Au, and Fig. 1 shows their top views. The 1/2 ML structure corresponds to a topmost copper-oxygen plane with Cu₂O stoichiometry on a (1×1) reconstruction of Cu₃Au(100) surface. We refer to this structure as $c(2 \times 2)$, and this nomenclature makes reference to the original fcc lattice of the pure systems (bulk Cu or Au). Accordingly, the 1/8 and 1/18 ML structures correspond to (2×2) and (3×3) supercells of the Cu₃Au(100) surface. Calculations for the isolated O₂ molecule (needed for the computation of adsorption energies) are performed with spin polarization.

We used $6 \times 6 \times 1$, $3 \times 3 \times 1$, and $2 \times 2 \times 1$ k -point samplings of a Monkhorst-Pack¹⁵ grid for 1/2 ML, 1/8 ML, and 1/18 ML, respectively. Only atomic positions of oxygen and surface copper atoms were optimized, the atomic coordinates for the three layers in the center of the slabs were kept fixed. The Cartesian forces at the atomic nuclei were minimized until 0.001 Ry/bohr. For the simulations of STM images, we used Tersoff-Hamann approximation in which the tunneling current is proportional to the local density of states (LDOS) at the position of the tip, integrated in the bias.^{16,17} We use 0.1 eV above the Fermi level (empty states) as the energy window for integrating the LDOS for simulated STM images. The images for filled states in the corresponding energy range look identical. Slab and isosurface images were generated by XCRYSDEN.¹⁸

IV. RESULTS AND DISCUSSION

Our experimental STM results are presented in Fig. 2, which shows the surface before and after oxygen implantation and annealing. These results are in accordance with the findings of Niehus and Achete³ for the O/Cu₃Au(100)- $c(2 \times 2)$ structure. Our STM data provide a corrugation of 0.032 nm. As we mentioned previously, from the STM images alone one cannot assign the bright spots in the images to any specific atomic species. However, as we also mentioned, based on previous knowledge for isolated O impurities, one would be tempted to assign the bright spots (dark circles) to Cu and the dark sites (white circles) to the O positions.

This uncertainty is resolved with the help of our *ab initio* calculations. Initially, we search for the most stable oxygen arrangement for 1/2 ML coverage by testing the fourfold hollow sites above subsurface Cu atoms or Au atoms. The most stable structure is the former, in agreement with Niehus and Achete,³ and the calculated energy difference is 0.50 eV per oxygen atom. The calculated Cu-O distance is 1.92 Å, close the value of 1.97 Å obtained by Kangas *et al.* for O/Cu(100).¹⁹

Then, we compute the adsorption energy per oxygen atom as a function of coverage as

$$\Delta E = (E_{O/Cu_3Au} - E_{Cu_3Au} - E_{O_2})/2, \quad (1)$$

where E_{O/Cu_3Au} is the energy of the O/Cu₃Au slab, E_{Cu_3Au} is the energy of the clean Cu₃Au surface slab, and E_{O_2} of an

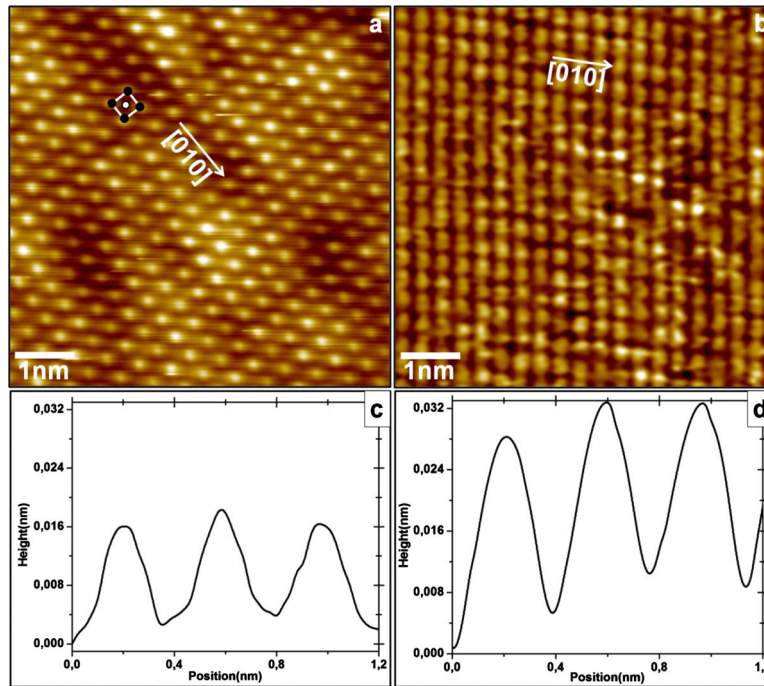


FIG. 2. (Color online) STM images for (a) clean $\text{Cu}_3\text{Au}(100)$ surface ($U_{\text{tip}}=-150$ mV; $I_t=0.5$ nA) and (b) $\text{O}/\text{Cu}_3\text{Au}(100)$ surface ($U_{\text{tip}}=-20$ mV; $I_t=2.2$ nA), with $1/2$ ML of oxygen atoms. In panels (c) and (d), are height profiles obtained along the $[010]$ direction of the clean and O-terminated surfaces, respectively.

isolated O_2 molecule. The factor of $1/2$ accounts for the fact that we have a symmetric slab, with one oxygen atom in each surface. Our calculations yield adsorption energies of -2.67 eV, -2.57 eV, and -2.75 eV for $1/2$ ML, $1/8$ ML, and $1/18$ ML coverages, respectively, indicating that the $\text{O}/\text{Cu}_3\text{Au}(100)$ surface is strongly stable.²⁰ Moreover, the adsorption energy for $1/18$ ML coverage is more negative than that of $1/8$ ML coverage, indicating an effectively repulsive interaction between oxygen atoms in the isolated-impurity regime, similarly to what has been found for $\text{O}/\text{Cu}(100)$.¹⁹ However, the $1/2$ ML structure seems to be particularly stable, having a more negative adsorption energy than the $1/8$ ML structure. That may indicate important changes in the electronic structure of the surface when we go from the isolated impurity to the oxide regimes, as we will further demonstrate below by analysis of the simulated STM images.

Figure 3(a) shows our simulated constant-height STM images for $1/2$ ML oxygen coverage where, surprisingly, the LDOS maxima (bright spots) are located above the oxygen

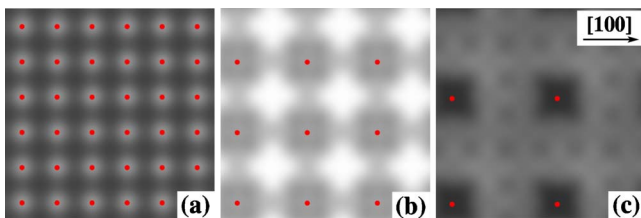


FIG. 3. (Color online) Simulated STM for (a) $1/2$ ML, (b) $1/8$ ML, and (c) $1/18$ ML coverages. The projected positions of the oxygen atoms are marked with red dots.

atoms (red dots) and not above the copper atoms. Therefore, the bright spots in our experimental images (Fig. 2) are assigned to oxygen atoms. To reconcile this result with the well-known behavior of isolated oxygen impurities, we performed similar simulations for $1/8$ and $1/18$ ML oxygen atom coverages, shown in Figs. 3(b) and 3(c). Then, the expected result is obtained. The oxygen atoms appear as minima (dark spot) in the LDOS plot. In particular, for the lowest calculated coverage, the isolated oxygen STM image appears like a dark square, in analogy of the experimental data obtained for oxygen low coverage on $\text{Cu}(111)$ by Wiame *et al.*⁷ where the oxygen atoms were identified at the center of dark triangles. This is consistent with the fact that $\text{Cu}_3\text{Au}(100)$ has a C_4 symmetry axis and $\text{Cu}(111)$ has a C_3 symmetry axis. Therefore, oxygen atoms appear as bright spots in the high-coverage (oxide) regime and as dark spots in the low-coverage (isolated-impurity) regime.

We can further understand this behavior by analyzing the cross-sectional integrated LDOS, shown in Fig. 4. One

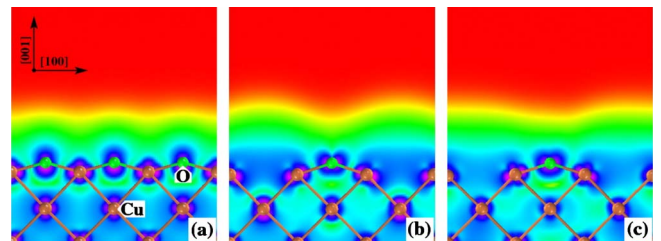


FIG. 4. (Color online) Integrated local density of states for (a) $1/2$ ML, (b) $1/8$ ML, and (c) $1/18$ ML coverages. The color code goes from red to purple as the density increases.

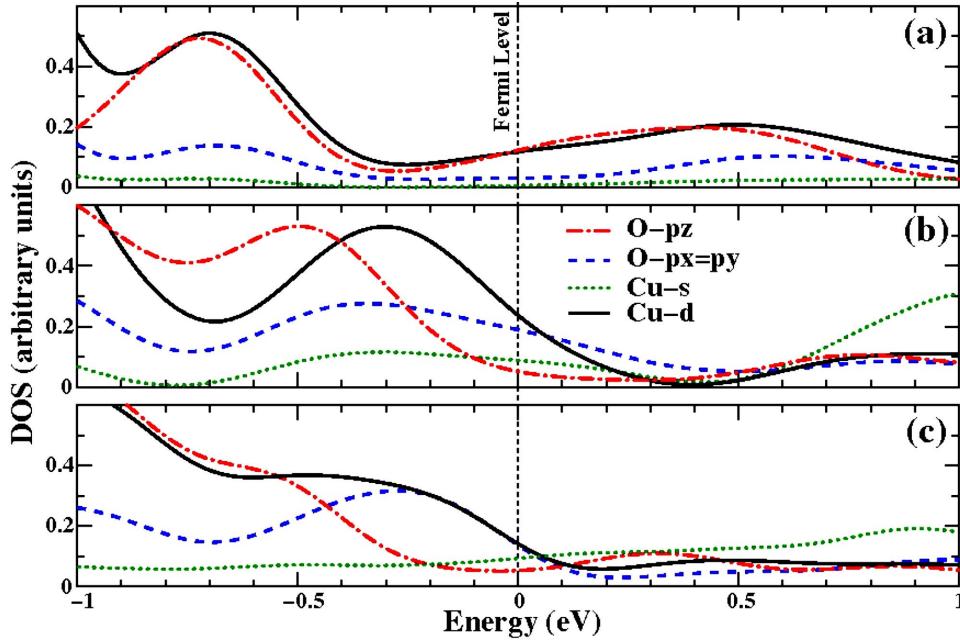


FIG. 5. (Color online) Projected DOS into atomic orbitals for (a) 1/2 ML, (b) 1/8 ML, and (c) 1/18 ML coverage.

clearly notices that the LDOS near the oxygen atom resembles p_z atomic orbitals sticking out of the surface for 1/2 ML coverage, giving rise to a bright STM spot. On the other hand, for lower coverages, the oxygen atomic character of the Fermi-level states appears to be (p_x, p_y) -like, producing a dark STM spot. This is further confirmed by projecting out the energy eigenstates into atomic orbitals, as shown in Fig. 5. In the oxide regime [Fig. 5(a)], the states at the Fermi level have mostly $O(p_z)$ and $Cu(d)$ character so the STM images are dominated by the former. In the isolated-impurity limit [Figs. 5(b) and 5(c)], the oxygen character of the Fermi-level states changes to $O(p_x, p_y)$. Therefore, the change in STM signatures from impurity to oxide regimes is can be traced back to a change in the oxygen orbital character of the Fermi-level states.

V. CONCLUSIONS

In conclusion, the STM signatures of the oxygen atom in $Cu_3Au(100)$ surfaces show an interesting and nontrivial cov-

erage dependence, appearing as depressions (dark spots) in the isolated-impurity regime (low coverage) and as protrusions (bright spots) in the oxide regime (high coverage). A change in the orbital character of the Fermi-level states at the oxygen atoms is responsible for this effect. This behavior could very well occur in other metallic surfaces, and one then should be careful to interpret STM measurements for high coverage based on the behavior of isolated impurities. Moreover, the theoretical simulation and understanding of STM images resulted in the chemical identification by STM of oxygen and copper atoms in the fully ordered $O/Cu_3Au(100)-c(2 \times 2)$ surface.

ACKNOWLEDGMENTS

This work was supported by Brazilian agencies CNPq, FAPERJ, and FINEP.

*Corresponding author; alexandre.leitao@ufjf.edu.br

¹M. Okada, K. Moritani, T. Fukuyama, H. Mizutani, A. Yoshigoe, Y. Teraoka, and T. Kasai, *Surf. Sci.* **600**, 4228 (2006).

²M. Okada, M. Hashinokuchi, M. Fukuoka, T. Kasai, K. Moritani, and Y. Teraoka, *Appl. Phys. Lett.* **89**, 201912 (2006).

³H. Niehus and C. A. Achete, *Surf. Sci.* **289**, 19 (1993).

⁴L. G. Dias and A. A. Leitão, C. A. Achete, R. P. Blum, H. Niehus, and R. B. Capaz, *Surf. Sci.* **601**, 5540 (2007).

⁵J. Middeke, R.-P. Blum, M. Hafemeister, and H. Niehus, *Surf. Sci.* **587**, 219 (2005).

⁶J. Wintterlin, R. Schuster, and G. Ertl, *Phys. Rev. Lett.* **77**, 123 (1996).

⁷F. Wiame, V. Maurice, and P. Marcus, *Surf. Sci.* **601**, 1193 (2007).

⁸K. Yagyu, X. Liu, Y. Yoshimoto, K. Nakatsuji, and F. Komori, *J. Phys. Chem. C* **113**, 5541 (2009).

⁹T. Fujita, Y. Okawa, Y. Matsumoto, and K. I. Tanaka, *Phys. Rev. B* **54**, 2167 (1996).

¹⁰P. Hohenberg and W. Kohn, *Phys. Rev.* **136**, B864 (1964).

¹¹W. Kohn and L. J. Sham, *Phys. Rev.* **140**, A1133 (1965).

¹²J. P. Perdew and A. Zunger, *Phys. Rev. B* **23**, 5048 (1981).

¹³D. Vanderbilt, *Phys. Rev. B* **41**, 7892 (1990).

¹⁴P. Giannozzi, S. Baroni, N. Bonini, M. Calandra, R. Car, C. Cavazzoni, D. Ceresoli, G. L. Chiarotti, M. Cococcioni, I. Dabo, A. Dal Corso, S. de Gironcoli, S. Fabris, G. Fratesi, R. Gebauer, U. Gerstmann, C. Gougoussis, A. Kokalj, M. Lazzeri, L. Martin-Samos, N. Marzari, F. Mauri, R. Mazzarello, S. Paolini, A. Pasquarello, L. Paulatto, C. Sbraccia, S. Scandolo, G. Sclauzero,

- A. P. Seitsonen, A. Smogunov, P. Umari, and R. M. Wentzcovitch, *J. Phys.: Condens. Matter* **21**, 395502 (2009).
- ¹⁵H. Monkhorst and J. Pack, *Phys. Rev. B* **13**, 5188 (1976).
- ¹⁶J. Tersoff and D. R. Hamann, *Phys. Rev. Lett.* **50**, 1998 (1983).
- ¹⁷J. Tersoff and D. R. Hamann, *Phys. Rev. B* **31**, 805 (1985).
- ¹⁸A. Kokalj, *Comput. Mater. Sci.* **28**, 155 (2003); code available from <http://www.xcrysden.org>
- ¹⁹T. Kangas, K. Laasonen, A. Puisto, H. Pitkänen, and M. Alatalo, *Surf. Sci.* **584**, 62 (2005).
- ²⁰This is in apparent contrast to the experimentally observed inertness of the Cu₃Au(100) surface under molecular oxygen adsorption. However, one has to keep in mind that the pure Cu₃Au(100) surface is Cu-Au terminated and the presence of gold atoms is certainly decisive to render the surface inert. In other words, Eq. (1) should not be used to describe the energetics of the O/Cu₃Au(100) formation but it gives rather a good estimate of the surface stability for O desorption.